

unstrained aminocycloalkanes remains challenging, probably due to the high reverse cyclization rate and the insufficient ring strain.⁷ Therefore, the exploration of new strategies for unstrained C–C bond cleavage is still important and desirable.

Aromatization is recognized as one of the most important thermodynamic driving forces for many chemical transformations.⁸ Especially in radical chemistry, the aromatization-driven cleavage of chemical bonds is an important transformation. In this field, structurally diverse pre-aromatic (PA) compounds such as 1,4-DHPs,⁹ benzothiazolines,¹⁰ dihydroquinazolinones,¹¹ and others¹² are widely used as hydrogen atom transfer (HAT) reagents, functional group transfer reagents and radical precursors. For example, Dong and co-workers disclosed several unique deacylative C–C bond functionalizations of chain ketones,¹³ in which the *in situ* formed pre-aromatic intermediates underwent Ir(III)-catalyzed aromatization-driven C–C bond cleavage to achieve the deacylation process. Recently, Martin,¹⁴ Zhu¹⁵ and others¹⁶ reported a series of photoredox-catalyzed radical alkylation reactions by using 2,3-dihydroquinazolinones as efficient alkyl radical precursors. However, large amounts of quinazolinones were formed as by-products, which may be against the concept of green synthesis. Despite these reports, the aromatization-driven C–C bond cleavage of unstrained carbocycles remains unexplored. As mentioned above, the cyclic C–C bond cleavage induced by nitrogen-centered radicals is usually limited to

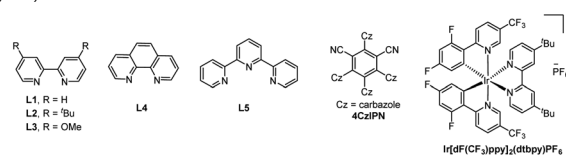
strained rings. Therefore, we set out to embed this aminocycloalkane skeleton in a latent aromatic molecule, hoping that the strong driving force of aromatization would facilitate the cleavage of the less strained C–C bond (Scheme 1b). Here, we demonstrate a dual photoredox- and nickel-catalyzed deconstructive cross-coupling of spiro 2,3-dihydroquinazolin-4(1H)-ones with organic halides *via* nitrogen-centered radical-triggered β -scission (Scheme 1c). The noteworthy features of this study include: (1) the mild and redox-neutral reaction conditions, the practical scalability and the use of inexpensive, commercially available 4CzIPN as the organic photocatalyst, which make this protocol of great potential in organic synthesis; (2) this method exhibits broad substrate scope (aryl, alkenyl, alkynyl and alkyl bromides) and excellent functional group compatibility; (3) most remarkably, the useful quinazolinone fragments generated *in situ* were successfully retained in the final product, exhibiting excellent atom efficiency.¹⁷

To verify our hypothesis, spiro 2,3-dihydroquinazolin-4(1H)-one **1a** was first prepared by condensation of 2-methyl cyclopentanone with 2-aminobenzamide. Then, the reaction of **1a** with aryl bromide **2a** was chosen as a model reaction to find the optimal conditions (Table 1). We were pleased to find that the reaction proceeded successfully in the presence of 4CzIPN (1 mol%), NiCl₂·DME (10 mol%), dtbpy (**L2**, 12 mol%), and K₂CO₃ in DMF under 10 W blue LED irradiation, yielding the desired ring-opening/coupling product **3a** in 73% yield. The

Table 1 Optimization of the reaction conditions^a



Entry	Variation from standard conditions	Yield of 3a ^b /%	Yield of 3a' ^b /%
1	None	73	9
2	Ni(COD) ₂ instead of NiCl ₂ ·DME	18	12
3	NiCl ₂ instead of NiCl ₂ ·DME	45	18
4	L1 instead of L2	55	13
5	L3 instead of L2	72	10
6	L4 instead of L2	61	17
7	L5 instead of L2	37	11
8	DMSO as solvent	81	<5
9	DMAc, NMP, and MeCN as solvent	71/68/46	10
10	4CzPN instead of 4CzIPN	75 ^c	<5
11	Ir[dF(CF ₃)ppy] ₂ (dtbpy)PF ₆ as PC	66 ^c	<5
12	Na ₂ CO ₃ as the base	83 ^c	<5
13	2,4,6-Colidine as the base	80 ^c	<5
14	1.5 equiv. of 1a was used	90 ^c	<5
15	No pc, [Ni], L2 , base or in darkness	Trace ^c	Trace



^a Reaction conditions: **1a** (0.24 mmol, 1.2 equiv.), **2a** (0.2 mmol, 1.0 equiv.), 4CzIPN (1.0 mol%), NiCl₂·DME (10 mol%), dtbpy (12 mol%) and K₂CO₃ (1.0 equiv.) in DMF (2.0 mL) with 10 W blue LEDs irradiation at room temperature for 12 h under N₂. ^b Isolated yields. ^c DMSO was used as solvent.



Table 2 Scope of organic halides^a

^a Reaction conditions: spiro dihydroquinazolinone **1a** (0.3 mmol, 1.5 equiv.), aryl bromides **2** (0.2 mmol, 1.0 equiv.), 4CzIPN (1 mol%), NiCl₂·DME (10 mol%), **L2** (12 mol%), K₂CO₃ (1.0 equiv.), and DMSO (2.0 mL) with 10 W blue LEDs irradiation at room temperature for 12 h under N₂. Isolated yields.

screening of nickel catalysts and ligands showed that the combination of NiCl₂·DME and **L2** was the most efficient, giving the best yield of **3a** (entries 2–7). Solvent screening showed that polar solvents were more suitable, giving **3a** in moderate to good yields and DMSO was the optimal solvent (entries 8 and 9). Both Ir-based complex and organic photocatalysts were evaluated for this transformation, with 4CzIPN still being the best (entries 10 and 11). Inorganic bases such as Na₂CO₃ and organic bases such as 2,4,6-collidine both gave a comparable yield of **3a** (entries 12 and 13). Satisfactorily, increasing the amount of **1a** from 1.2 equiv. to 1.5 equiv. led to an improved 90% yield of **3a** (entry 14). Control experiments showed that the photocatalyst, nickel catalyst, ligand, base and visible-light irradiation were all essential for this transformation (entry 15). Finally, it should be mentioned that a certain amount of ring-opening/HAT product **3a'** was also detected during the optimization.

With the optimized conditions established, the generality and limitations of aryl bromides for this deconstructive arylation reaction were first evaluated. As shown in Table 2, a number of aryl bromides reacted efficiently with **1a** under standard conditions to afford the target products **3a–l** in good to excellent yields. The electronic and steric effects on the aromatic moiety showed a significant influence on the reaction efficiency. In general, aryl bromides with strong electron-withdrawing groups on the *para* position of the aromatic ring gave better yields (**3a–h** vs. **3i** and **3j**). Satisfactorily, a wide range of functional groups including acetyl (**3a** and **3k**),

methylsulfonyl (**3b**), ester (**3c**), formyl (**3d**), cyano (**3e**), trifluoromethyl (**3f**), benzoyl (**3g**) and chloro (**3h** and **3l**) groups were well tolerated in this reaction. 5-Bromoindanone and 5-bromophthalide also afforded the desired products **3m** and **3n** in good yields. Heteroaromatic bromides, such as 3-bromoquinoline, 6-bromoquinoline and 4-bromopyridine, were also amenable and afforded the target products **3o–q** in moderate yields. In addition to aryl bromides, vinyl bromide (**3s**) and alkynyl bromide (**3t**) were also applicable to this protocol. Remarkably, aryl bromides masked by natural products or drugs also participated well in this coupling reaction, giving the expected products (**3v–z**) in satisfactory yields. These results highlighted the application potential of this protocol in the diversification of natural products and pharmaceuticals.

Subsequently, the scope of spiro dihydroquinazolinones derived from various cycloalkanones and 2-aminobenzamides was investigated using aryl bromide **2a** as a model coupling partner. As shown in Table 3, various dihydroquinazolinones derived from 2-substituted cyclopentanones were all efficiently engaged in this C–C bond cleavage/coupling to afford the products **5a–l** in 55–91% yields. Substrates derived from nor-camphors and loxoprofen also afforded the desired products **5e–g** in good yields. Dihydroquinazolinones with a methyl protecting group on the amide moiety showed better reaction efficiency, giving the product **5h** in 91% yield. Dihydroquinazolinones with different substituents on the aromatic rings also reacted efficiently with **2a** to afford the products **5i–l** in moderate yields. Meanwhile the substrate with a 5-Me group on the aromatic ring gave the desired product **5j** in only 20% yield, due to low conversion. It was found that the existence of a 2-substituent on the aliphatic ring is very crucial for the success of this transformation, probably due to its stabilizing

Table 3 Scope of dihydroquinazolinone^a

^a Reaction conditions: dihydroquinazolinone **1** (0.3 mmol, 1.5 equiv.), aryl halides **2a** (0.2 mmol, 1.0 equiv.), 4CzIPN (1 mol%), NiCl₂·DME (10 mol%), **L2** (12 mol%), K₂CO₃ (1.0 equiv.), and DMSO (2.0 mL) with 10 W blue LEDs irradiation at room temperature for 12 h under N₂. Isolated yields.



effect on the alkyl radical intermediates. Substrates derived from simple cyclopentanone and 2,2-dimethylcyclopentanone both failed to give the product. For the former, the rapid reverse 5-*exo* cyclization was probably the main reason. For the latter, the steric hindrance of the tertiary radical generated *in situ* made the coupling reaction more difficult. Notably, the substrate derived from cyclobutanone was efficient, giving the desired product **5m** in 88% yield. For the six-membered ring systems, the 2-phenoxy-substituted substrate was successfully converted to the expected product **5n** in 80% yield, while the 2-methyl analogue was inactive.

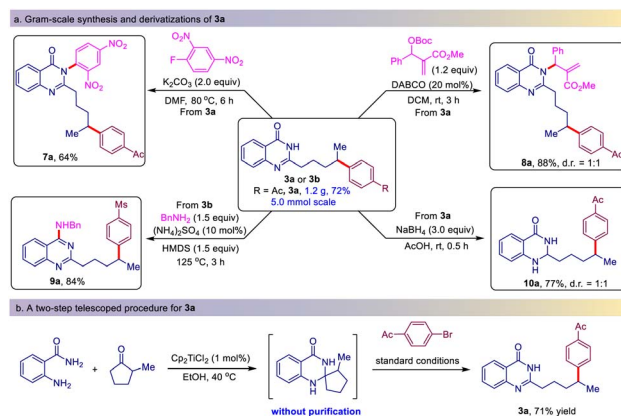
It is known that the nucleophilicity and lifetime of alkyl radicals can be influenced by the electronegativity and the π -bonding capability of the α -heteroatom.¹⁸ Therefore, we intend to evaluate the influence of the heteroatom on this C–C bond cleavage/coupling reaction (Table 4). We introduced oxygen and nitrogen atoms into aliphatic ring systems, respectively. Fortunately, the substrate derived from dihydrofuran-3(2*H*)-one successfully underwent this ring-opening/coupling reaction to give the expected product **6a** in 86% yield with excellent regioselectivity. The substrate generated from *N*-Cbz-pyrrolidin-3-one also worked well with **2a** to afford the product **6b** in 74% yield. In addition to the five-membered system, the six-membered analogues were also compatible for this transformation (**6c** and **6d**). Remarkably, the coupling partners can be further extended to alkyl halides (**6e–i**). A variety of functional groups such as cyano (**6f**), alkynyl (**6g**), alkenyl (**6h**), and phthalimide (**6i**) were all tolerated in this transformation.

To demonstrate the applicability of this protocol, the gram-scale synthesis of **3a** and its derivatizations were carried out (Scheme 2a). When the model reaction was scaled up to the 5.0 mmol scale, the reaction still proceeded smoothly to give **3a** in a slightly reduced but acceptable yield (1.2 g, 72% yield). The

Table 4 Scope of dihydroquinazolinone^a

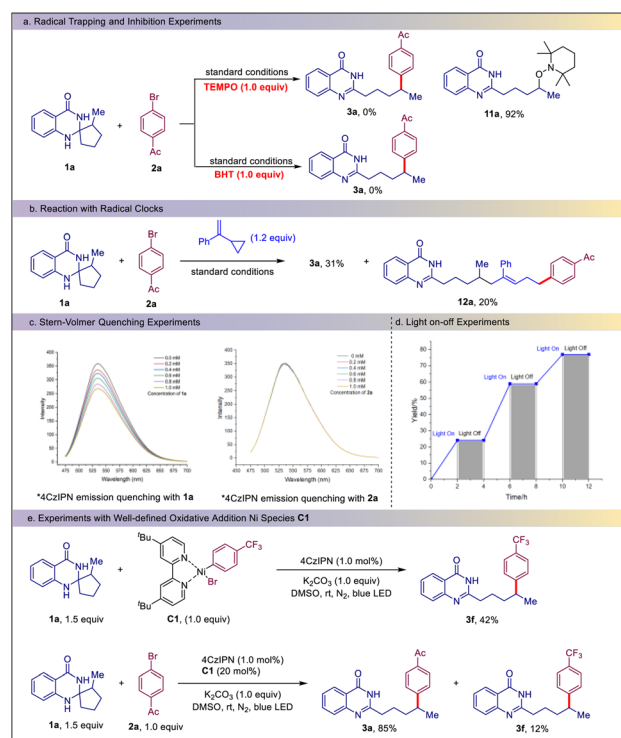


^a Reaction conditions: dihydroquinazolinone **1** (0.3 mmol, 1.5 equiv.), aryl halides **2** or **4** (0.2 mmol, 1.0 equiv.), 4CzIPN (1 mol%), NiCl₂·DME (10 mol%), L2 (12 mol%), K₂CO₃ (1.0 equiv.), and DMSO (2.0 mL) with 10 W blue LEDs irradiation at room temperature for 12 h under N₂. Isolated yields.



Scheme 2 Application investigation.

derivatization of **3a** was then investigated. **3a** can undergo nucleophilic substitution with 2,4-dinitrofluorobenzene to give the *N*-aryl product **7a** in 64% yield. It also reacted with Morita–Baylis–Hillman ester to give the *N*-allylic product **8a** in 88% yield. In addition, quinazolin-4(3*H*)-one **3b** underwent a HMDS-mediated amination reaction with benzylamine to afford 4-aminoquinazolinone **9a** in 84% yield. Finally, the treatment of **3a** with NaBH₄ afforded the unexpected dearomatized product **10a** in 77% yield as the sole product. To further increase the synthetic utility of this protocol, we telescoped the formation of spiro dihydroquinazolinones and the ring-opening/coupling reaction without purification (Scheme 2b). Satisfactorily, the 2-



Scheme 3 Mechanism studies.



methylcyclopentanone efficiently underwent this two-step process and afforded **3a** in 71% isolated yield.

To gain mechanistic insight into this reaction, some control experiments were performed (Scheme 3). It was found that the reaction of **1a** and **2a** was totally inhibited by the addition of 1.0 equiv. of TEMPO. In this case, the TEMPO adduct **11a** was isolated in 92% yield. The addition of 1.0 equiv. of BHT also completely suppressed the reaction (Scheme 3a). These results indicated that the reaction proceeded *via* a radical pathway. When (1-cyclopropylvinyl)benzene was added to the reaction system, in addition to 31% of product **3a**, the three-component product **12a** was isolated in 20% yield, providing further evidence for a radical pathway (Scheme 3b). Stern–Volmer fluorescence quenching experiments showed that the excited 4-CzIPN* was effectively quenched by the dihydroquinazolinone **1a** rather than the bromide **2a**, suggesting that an excited state charge transfer occurred between 4-CzIPN* and **1a** (Scheme 3c). Light on and off experiments showed that continuous irradiation is essential for this transformation (Scheme 3d and see also the ESI†). To elucidate the Ni catalytic cycle, an isolated Ni(II) complex **C1** was prepared in advance and then treated with **1a** under the standard conditions. As expected, the product **3f** could be obtained in 42% yield. Furthermore, the use of Ni(II) complex **C1** as a catalyst for the reaction of **1a** and **2a** also led to the formation of **3a** in 85% yield, along with 12% yield of **3f** (Scheme 3e). These results suggest that the Ar–Ni(II) complex is a key intermediate in the Ni-catalytic cycle.

Based on the above experimental results and previous literature,¹⁹ a possible mechanism for this ring-opening/coupling is proposed (Scheme 4). First, 4CzIPN is photoexcited to its excited state 4CzIPN*, which is a sufficient SET oxidant. Then, single electron oxidation of dihydroquinazolinone **1a** by the photoexcited 4CzIPN* yields the aminyl radical cation **I** and the radical anion [4CzIPN]^{•−}. In the presence of a base, the radical cation intermediate **I** undergoes aromatization driven β-scission to give the alkyl radical **II**. Concurrently, the oxidative addition of aryl bromide **2a** to active Ni(0)Ln produces the Ni(II) species **III**. Radical recombination of the Ni(II) species **III** with the alkyl radical **II** yields the Ni(III) species **IV**, which undergoes reductive elimination to give the target product **3a** and the LnNi(I)Br species **V**. Finally, the two catalytic cycles are completed

simultaneously by a single electron transfer between the [4CzIPN]^{•−} radical anion and LnNi(I)Br **V**, regenerating both the active Ni(0)Ln species and 4CzIPN.

Conclusions

In summary, we have developed a novel aromatization-driven deconstructive cross-coupling of spiro dihydroquinazolinones *via* dual photoredox/nickel catalysis. This is the first example of aromatization-driven nitrogen-centered radical-induced cyclic C–C bond cleavage. In contrast to previous reports, this strategy allows the aromatic fragments formed *in situ* *via* C–C bond cleavage to be successfully retained in the product. Under the synergistic photoredox/nickel catalysis, the deconstructive coupling of spiro dihydroquinazolinones with various organic halides, including aryl, alkenyl, alkynyl and alkyl bromides, proceeded efficiently to afford a series of useful functionalized quinazolinones in good yields with excellent functional group tolerance. An in-depth mechanism study revealed that this reaction proceeded *via* a radical-metal crossover pathway. This work provides a complementary strategy for the radical-mediated C–C bond cleavage of unstrained carbocycles.

Data availability

All experimental and characterization data including NMR spectra are available in the ESI†

Author contributions

H.-J. Miao performed all the experiments and prepared the manuscript and ESI.† J.-H. Zhang, W. Li, W. Yang and H. Xin performed the preparation of raw materials. X.-H. Duan and L.-N. Guo directed this project and revised the manuscript. All authors have given approval to the final version of the manuscript.

Conflicts of interest

There are no conflicts to declare.

Acknowledgements

Financial support from the National Natural Science Foundation of China (No. 22171220, 21971201) and the Fundamental Research Funds of the Central Universities (No. xtr072022003) is greatly appreciated. We also thank Mr Zhang, Miss Feng and Miss Bai at the Instrument Analysis Center of Xi'an Jiaotong University for their assistance with NMR and HRMS analysis.

Notes and references

- For selected reviews, see: (a) F. Song, T. Gou, B.-Q. Wang and Z.-J. Shi, *Chem. Soc. Rev.*, 2018, **47**, 7078–7115; (b) Y. Xue and G. Dong, *Acc. Chem. Res.*, 2022, **55**, 2341–2354; (c) F. Song, B. Wang and Z.-J. Shi, *Acc. Chem. Res.*, 2023, **56**, 2867–2886.



Scheme 4 Proposed Mechanism.



- 2 For selected reviews, see: (a) X. Wu and C. Zhu, *Chem. Commun.*, 2019, **55**, 9747–9756; (b) P. Sivaguru, Z. Wang, G. Zanoni and X. Bi, *Chem. Soc. Rev.*, 2019, **48**, 2615–2656; (c) E. Tsui, H. Wang and R. R. Knowles, *Chem. Sci.*, 2020, **11**, 11124–11141; (d) X.-Y. Yu, Q.-Q. Zhao, J. Chen, W.-J. Xiao and J.-R. Chen, *Acc. Chem. Res.*, 2020, **53**, 1066–1083; (e) S.-H. Shi, Y. Liang and N. Jiao, *Chem. Rev.*, 2021, **121**, 485–505; (f) X.-Y. Yu, J.-R. Chen and W.-J. Xiao, *Chem. Rev.*, 2021, **121**, 506–561; (g) L. Chang, Q. An, L. Duan, K. Feng and Z. Zuo, *Chem. Rev.*, 2022, **122**, 2429–2486.
- 3 For recent examples: (a) H. Zhao, X. Fan, J. Yu and C. Zhu, *J. Am. Chem. Soc.*, 2015, **137**, 3490–3493; (b) H. G. Yayla, H. Wang, K. T. Tarantino, H. S. Orbe and R. R. Knowles, *J. Am. Chem. Soc.*, 2016, **138**, 10794–10797; (c) L. Huang, T. Ji and M. Rueping, *J. Am. Chem. Soc.*, 2020, **142**, 3532–3539; (d) S. Sakurai, A. Matsumoto, T. Kano and K. Maruoka, *J. Am. Chem. Soc.*, 2020, **142**, 19017–19022; (e) Y. Chen, J. Du and Z. Zuo, *Chem*, 2020, **6**, 266–279; (f) L. Wen, J. Ding, L. Duan, S. Wang, Q. An, H. Wang and Z. Zuo, *Science*, 2023, **382**, 458–464.
- 4 For selected examples: (a) J. Boivin, E. Fouquet and S. Z. Zard, *J. Am. Chem. Soc.*, 1991, **113**, 1057–1059; (b) T. Nishimura, T. Yoshinaka, Y. Nishiguchi, Y. Maeda and S. Uemura, *Org. Lett.*, 2005, **7**, 2425–2427; (c) L. Li, H. Chen, M. Mei and L. Zhou, *Chem. Commun.*, 2017, **53**, 11544–11547; (d) B. Zhao and Z. Shi, *Angew. Chem., Int. Ed.*, 2017, **56**, 12727–12731; (e) X.-Y. Yu, J.-R. Chen, P.-Z. Wang, M.-N. Yang, D. Liang and W.-J. Xiao, *Angew. Chem., Int. Ed.*, 2018, **57**, 738–743; (f) E. M. Dauncey, S. P. Morcillo, J. J. Douglas, N. S. Sheikh and D. Leonori, *Angew. Chem., Int. Ed.*, 2018, **57**, 744–748; (g) J. Chen, Y.-J. Liang, P.-Z. Wang, G.-Q. Li, B. Zhang, H. Qian, X.-D. Huan, W. Guan, W.-J. Xiao and J.-R. Chen, *J. Am. Chem. Soc.*, 2021, **143**, 13382–13392.
- 5 (a) S. Wang, L.-N. Guo, H. Wang and X.-H. Duan, *Org. Lett.*, 2015, **17**, 4798–4801; (b) Y.-R. Gu, X.-H. Duan, L. Yang and L.-N. Guo, *Org. Lett.*, 2017, **19**, 5908–5911; (c) J.-J. Zhang, X.-H. Duan, Y. Wu, J.-C. Yang and L.-N. Guo, *Chem. Sci.*, 2019, **10**, 161–166; (d) J.-C. Yang, L. Chen, F. Yang, P. Li and L.-N. Guo, *Org. Chem. Front.*, 2019, **6**, 2792–2795; (e) L. Chen, L.-N. Guo, S. Liu, L. Liu and X.-H. Duan, *Chem. Sci.*, 2021, **12**, 1791–1795; (f) L. Liu, X.-H. Duan and L.-N. Guo, *Synthesis*, 2021, **57**, 4375–4388; (g) S. Liu, P. Ma, L. Zhang, S. Shen, H.-J. Miao, L. Liu, K. N. Houk, X.-H. Duan and L.-N. Guo, *Chem. Sci.*, 2023, **14**, 5220–5225; (h) Q.-C. Shan, Y. Zhao, S.-T. Wang, H.-F. Liu, X.-H. Duan and L.-N. Guo, *ACS Catal.*, 2024, **14**, 2144–2150.
- 6 (a) S. Maity, M. Zhu, R. S. Shinabery and N. Zheng, *Angew. Chem., Int. Ed.*, 2012, **51**, 222–226; (b) S. A. Morris, J. Wang and N. Zheng, *Acc. Chem. Res.*, 2016, **49**, 1957–1968; (c) D. M. Arias-Rotondo and J. K. McCusker, *Chem. Soc. Rev.*, 2016, **45**, 5803–5820; (d) Y. Cai, J. Wang, Y. Zhang, Z. Li, D. Hu, N. Zheng and H. Chen, *J. Am. Chem. Soc.*, 2017, **139**, 12259–12266; (e) M.-M. Wang and J. Waser, *Angew. Chem., Int. Ed.*, 2019, **58**, 13880–13884; (f) M.-M. Wang, T. V. T. Nguyen and J. Waser, *Chem. Soc. Rev.*, 2022, **51**, 7344–7357.
- 7 (a) J.-W. Zhang, Y.-R. Wang, J.-H. Pan, Y.-H. He, W. Yu and B. Han, *Angew. Chem., Int. Ed.*, 2020, **59**, 3900–3904; (b) C. Pratley, S. Fenner and J. A. Murphy, *Chem. Rev.*, 2022, **122**, 8181–8260.
- 8 A. Bhunia and A. Studer, *Chem*, 2021, **7**, 2060–2100.
- 9 (a) Á. Gutierrez-Bonet, J. C. Tellis, J. K. Matsui, B. A. Vara and G. A. Molander, *ACS Catal.*, 2016, **6**, 8004–8008; (b) K. Nakajima, S. Nojima, K. Sakata and Y. Nishibayash, *ChemCatChem*, 2016, **8**, 1028–1032; (c) W. Chen, Z. Liu, J. Tian, J. Li, J. Ma, X. Cheng and G. Li, *J. Am. Chem. Soc.*, 2016, **138**, 12312–12315; (d) J. A. Milligan, J. P. Phelan, S. O. Badir and G. A. Molander, *Angew. Chem., Int. Ed.*, 2019, **58**, 6152–6163; (e) H.-M. Huang, P. Bellotti, C. G. Daniliuc and F. Glorius, *Angew. Chem., Int. Ed.*, 2021, **60**, 2464–2471; (f) Y. Wei, B. Ben-zvi and T. Diao, *Angew. Chem., Int. Ed.*, 2021, **60**, 9433–9438.
- 10 (a) T. Uchikura, K. Moriyama, M. Toda, T. Mouri, I. Ibáñez and T. Akiyama, *Chem. Commun.*, 2019, **55**, 11171–11174; (b) T. Uchikura, M. Toda, T. Mouri, T. Fujii, K. Moriyama, I. Ibáñez and T. Akiyama, *J. Org. Chem.*, 2020, **85**, 12715–12723; (c) S.-C. Lee, L.-Y. Li, Z.-N. Tsai, Y.-H. Lee, Y.-T. Tsao, P.-G. Huang, C.-K. Cheng, H.-B. Lin, T.-W. Chen, C.-H. Yang, C.-C. Chiu and H.-H. Liao, *Org. Lett.*, 2022, **24**, 85–89; (d) T. Uchikura, N. Kamiyama, T. Mouri and T. Akiyama, *ACS Catal.*, 2022, **12**, 5209–5216.
- 11 (a) P. P. Mondal, A. Pal, A. K. Prakash and B. Sahoo, *Chem. Commun.*, 2022, **58**, 13202–13205; (b) X.-Y. Lv, R. Abrams and R. Martin, *Angew. Chem., Int. Ed.*, 2023, **62**, e202217386.
- 12 (a) M. Tian, X. Shi, X. Zhang and X. Fan, *J. Org. Chem.*, 2017, **82**, 7363–7372; (b) S.-C. Chen, Q. Zhu, Y. Cao, C. Li, Y. Guo, L. Kong, J. Che, Z. Guo, H. Chen, N. Zhang, X. Fang, J.-T. Lu and T. Luo, *J. Am. Chem. Soc.*, 2021, **143**, 14046–14052; (c) H. A. Sakai and D. W. C. MacMillan, *J. Am. Chem. Soc.*, 2022, **144**, 6185–6192; (d) S.-C. Chen, Q. Zhu, H. Chen, Z. Chen and T. Luo, *Chem.–Eur. J.*, 2023, **29**, e202203425.
- 13 (a) Y. Xu, X. Qi, P. Zheng, C. C. Berti, P. Liu and G. Dong, *Nature*, 2019, **567**, 373–378; (b) X. Zhou, Y. Xu and G. Dong, *Nat. Catal.*, 2021, **4**, 703–710; (c) X. Zhou, Y. Xu and G. Dong, *J. Am. Chem. Soc.*, 2021, **143**, 20042–20048; (d) X. Zhou, T. Yu and G. Dong, *J. Am. Chem. Soc.*, 2022, **144**, 9570–9575.
- 14 (a) X.-Y. Lv, R. Abrams and R. Martin, *Nat. Commun.*, 2022, **13**, 2394–2412; (b) F. Cong, R. S. Mega, J. Chen, C. S. Day and R. Martin, *Angew. Chem., Int. Ed.*, 2023, **62**, e202214633.
- 15 L. Li, L. Fang, W. Wu and J. Zhu, *Org. Lett.*, 2020, **22**, 5401–5406.
- 16 (a) P. P. Mondal, S. Das, S. Venugopalan, M. Krishnan and B. Sahoo, *Org. Lett.*, 2023, **25**, 1441–1446; (b) H. Wu, S. Chen, D. Xiao, F. Li, K. Zhou, X. Yin, C. Liu, X. He and Y. Shang, *Org. Lett.*, 2023, **25**, 1166–1171.
- 17 Quinazolinone fragments were widely existed in bioactive natural products and drugs, for selected examples, see: (a) R. Bouley, D. Ding, Z. Peng, M. Bastian, E. Lastochkin,



- W. Song, M. A. Suckow, V. A. Schroeder, W. R. Wolter, S. Mobashery and M. Chang, *J. Med. Chem.*, 2016, **59**, 5011–5021; (b) L. Hudson, J. Mui, S. Vázquez, D. M. Carvalho, E. Williams, C. Jones, A. N. Bullock and S. Hoelder, *J. Med. Chem.*, 2018, **61**, 7261–7272.
- 18 F. Parsaee, M. C. Senarathna, P. B. Kannangara, S. N. Alexander, P. D. E. Arche and E. R. Welin, *Nat. Rev. Chem.*, 2021, **5**, 486–499.
- 19 (a) J. C. Tellis, D. N. Primer and G. A. Molander, *Science*, 2014, **345**, 433–437; (b) A. Noble, S. J. McCarver and D. W. C. MacMillan, *J. Am. Chem. Soc.*, 2015, **137**, 624–627.

